Materials Today Sustainability 30 (2025) 101085

Contents lists available at ScienceDirect

Materials Today Sustainability

journal homepage: www.journals.elsevier.com/materials-today-sustainability

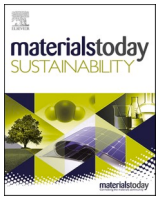

Sustainable CFRP drilling using support plates: A comprehensive analysis of delamination suppression and cost-effectiveness

Yun Seok Kang [a,1], Dong Eun Kim [b,1], Hyung Wook Park [a,*], Jaewoo Seo [b,**]

[a] Department of Mechanical Engineering, Ulsan National Institute of Science and Technology, UNIST-gil 50, Eonyang-eup, Ulju-gun, Ulsan, 44919, Republic of Korea
[b] Department of Mechanical Convergence Engineering, Gyeongsang National University, 48-54 Charyong-ro, Uichang-gu, Changwon, Gyeongnam, 51391, Republic of Korea

ARTICLE INFO

Keywords:
Carbon fiber-reinforced polymers
Drilling
Support plate
Machining economics

ABSTRACT

Carbon fiber-reinforced polymers (CFRPs) are extensively utilized in the aerospace industry due to their exceptional strength-to-weight ratios, enabling weight reduction and improved energy efficiency. Despite their advantages, the anisotropic properties of CFRPs result in defects, such as delamination, during drilling processes, reducing manufacturing efficiency and increasing production costs. While support plates have been employed to address such issues, existing studies have not sufficiently explored their economic and environmental implications, nor have they evaluated the potential of novel materials like cork. This study introduces a novel machining economics model tailored for CFRP drilling, integrating defect suppression, energy consumption, and production costs into a unified framework. Furthermore, this research uniquely explores cork as a support plate material, which has not been previously studied in the context of CFRP drilling. Experimental analyses demonstrate that cork achieves a 12.45% reduction in delamination and lowers overall drilling costs to 87.39% of those incurred without support plates. These findings establish cork as the most sustainable and cost-effective support plate material, while the proposed model provides a comprehensive method for evaluating machining quality and sustainability. By integrating a novel machining economics model and introducing cork as a support plate material, this study offers a practical solution to enhance cost-efficiency, defect suppression, and sustainability in aerospace manufacturing.

1. Introduction

With the advancement of the Fourth Industrial Revolution, sustainable production methods have become increasingly important [1–3]. Manufacturing plays a particularly crucial role in global economic growth, consuming approximately 25% of global industrial energy, of which approximately 11% is used by machine tools alone [4,5]. Moreover, CO_2 emissions are a major concern in the manufacturing industry, prompting extensive research on carbon reduction strategies [6–8]. Therefore, enhancing energy efficiency is essential for achieving carbon neutrality and sustainable manufacturing. Several factors such as the shape of the manufactured components, tool costs, and production time play vital roles in assessing the economic feasibility of manufacturing. Additionally, energy and resource consumption, along with labor costs during processing, affect productivity, making efficient production essential.

Carbon fiber-reinforced polymers (CFRPs) are composite materials composed of carbon fibers and a polymer matrix that are characterized by their high strength and stiffness, while remaining lightweight [9]. This lightweight nature provides an opportunity to reduce the overall energy consumption of structures, making them more efficient [10]. CFRPs are also resistant to chemical corrosion and maintain stability under a wide range of operating temperatures, making them well suited for aerospace industries that prioritize weight reduction and fuel efficiency [11]. This characteristic makes CFRPs a prominent eco-friendly material for reducing carbon emissions [12]. CFRP drilling processes are essential for assembly tasks such as riveting [13]. However, owing to the anisotropic, layered structure of CFRPs, drilling can result in damage such as delamination and uncut fibers at hole entrances and exits, potentially lowering machining quality and leading to part failure over

* Corresponding author.
** Corresponding author.
E-mail addresses: hwpark@unist.ac.kr (H.W. Park), jseo7717@gnu.ac.kr (J. Seo).
[1] Both Yun Seok Kang and Dong Eun Kim have contributed equally.

https://doi.org/10.1016/j.mtsust.2025.101085
Received 17 December 2024; Received in revised form 16 January 2025; Accepted 5 February 2025
Available online 13 February 2025

time. Such defects can increase rejection rates in the final stages of production by up to 60%, significantly increasing production costs [14, 15]. Various studies have proposed solutions to address these issues, such as optimizing the tool geometry [16], controlling the machining parameter [17–19], applying post-processing [20,21], and using support plates [22–24]. In particular, the use of support plates has gained attention as a straightforward approach for defect suppression because it involves simply attaching a support plate beneath the CFRP to effectively reduce defects. Dogrusadik et al. [25] used aluminum and wood support plates to investigate their influence on tool wear and defect reduction in the micro-drilling of CFRP laminates and found that aluminum support plates significantly decreased flank wear owing to their high rigidity, whereas wood plates provided moderate support, reducing delamination damage but with less impact on wear reduction. Kang et al. [26] applied various types of foam as cost-effective support plates to reduce delamination in CFRP drilling and analyzed the cutting forces and tool wear. Their results showed that using extruded polystyrene foam as a support plate reduced delamination by up to 35.9% compared with drilling CFRP without any support. Although studies have examined process improvements using support plates made of various materials, the economics and sustainability aspects of these methods remain underexplored.

Moreover, traditional models for evaluating machining economics typically include factors such as the machining, setup, and tooling cost [27–29]. Sustainable development requires the use of suitable materials across various industries to support a circular economy and low-carbon strategies. Makul [30] analyzed various techniques for low-carbon building materials and sustainable construction. Wang et al. [31] presented a model for predicting power consumption in drilling operations considering tool wear. The model reduced energy consumption and increased the tool usage. Khalid et al. [9] discussed ways to promote a circular economy and reduce environmental impacts through the recycling and reuse of synthetic materials. However, these models do not incorporate specific considerations for the unique characteristics of CFRP drilling, such as the layered structure and strict aerospace quality requirements. Recently, models have been proposed to assess additional processes, such as the use of cooling systems and lubricants, to improve both economic efficiency and environmental sustainability [32–37]. Nevertheless, these approaches are unsuitable for CFRP drilling due to the material's sensitivity to lubrication, leaving the development of a tailored economic model for dry machining processes unaddressed. Shah et al. [4] conducted a life cycle assessment of sustainable cutting fluid strategies for drilling Ti–6Al–4V, comparing cryogenic coolants (LCO_2 and LN_2) with conventional mineral-based flood coolants. Their evaluation considered the surface roughness, cutting energy, and energy efficiency, and the results indicated that cryogenic coolants enhanced energy efficiency and reduced environmental impact relative to conventional coolants. Race et al. [38] explore sustainable cooling in milling SA516 carbon steel, comparing flood coolant, dry machining, and minimum quantity lubrication (MQL). MQL proved environmentally beneficial, reducing tool wear, enhancing surface quality, and lowering energy use. It also minimized coolant disposal, offering cost savings and reduced environmental impact, highlighting its potential for heavy industries. Although these studies have made significant contributions, CFRP is typically drilled under dry conditions because its mechanical properties are degraded by the lubrication caused by hygroscopicity and resin expansion. This makes CFRPs difficult to machine. Furthermore, CFRP applications, particularly in aerospace components, demand high-quality parts with strict tolerances [39]; however, a comprehensive economic model that addresses these quality requirements has yet to be developed. Therefore, achieving a sustainable CFRP drilling process requires defect reduction and the development of a tailored model.

This study aims to enhance machinability by suppressing defects using support plates and proposes a sustainable CFRP drilling strategy through a machining economics model that reflects the drilling process outcomes, as shown in Fig. 1. Unlike previous studies, our model integrates defect suppression performance, energy consumption, and CO2 emissions into a unified framework, offering a comprehensive evaluation of economic and environmental sustainability. Our approach consists of machining experiments and sustainability assessments. The support plates used in the drilling process include Styrofoam, rubber, cork, and aluminum, each with unique mechanical and sustainability characteristics. Aluminum offers high strength and durability; rubber provides excellent flexibility and damping effects; foam is lightweight with superior damping properties and is easy to machine; and cork is an eco-friendly material with suitable strength and flexibility. Notably, cork, a renewable resource, possesses excellent mechanical properties that make it suitable for aerospace components, highlighting its potential applications in machining processes. The experimental results were analyzed to determine the effects of the support plates on thrust force

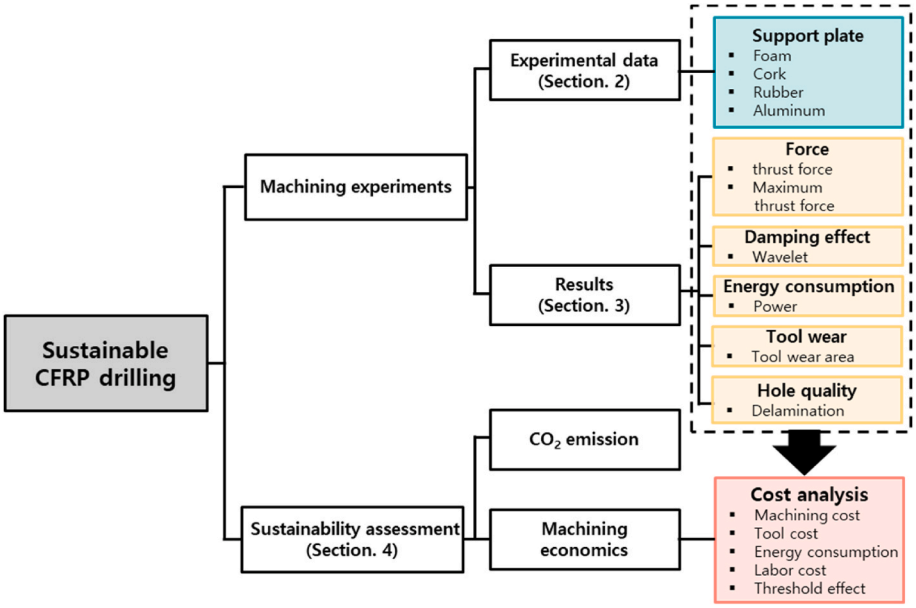

Fig. 1. Schematic of the research framework.

and tool wear during drilling, and the damping effect was evaluated using wavelet analysis. Energy consumption was also measured and derived from the power consumption during this process. Based on these results, a machining economics model was derived, along with a new economic model that incorporates a threshold for hole quality to ensure that the required quality standards are met. Additionally, CO_2 emissions were analyzed to comprehensively assess the sustainability of the drilling process.

2. Experimental setup

The drilling experiment was conducted using a three-axis computer numerical control machine (B 300, Hermle), as shown in Fig. 2. A power measurement module was installed to capture power data with a 0.2 s sampling rate using a digital power meter (Accura 2500, ROOTECH) following the ISO 14955 standard [40]. Additionally, an accelerometer (PCB 356A15, PCB Electronics) and a dynamometer (9256C2, Kistler) were attached to the jig to measure the vibrations and cutting forces during the process. The drilling tool used was a 4-mm-diameter solid carbide drill (Kennametal; B041A04000CPG) featuring a 30° helix angle and a 140° point angle. The machining conditions were set to a feed rate of 150 mm/min, spindle speed of 9000 RPM, and drilling depth of 10 mm to ensure complete penetration of the CFRP plate. The CFRP plates used in the experiment were fabricated from prepreg made of T300-reinforced fiber and epoxy resin (USN 150B, SK Chemicals). The detailed material properties are listed in Table 1. The drilling test dimensions were a width of 100 mm, length of 100 mm, and depth of 3 mm. Drilling was performed on each CFRP plate with 50 holes per plate, and four sets of tests were conducted, resulting in 200 holes being drilled under different support plate conditions. The support plates used were extruded polystyrene foam, rubber, cork, and aluminum, and their mechanical properties are listed in Table 2. The flexural strength and modulus were obtained via a three-point bending test, and the compressive modulus was obtained via a universal material compression test (Instron 5982, Instron). During drilling, the support plates were attached directly beneath the CFRP plate and fixed to the jig. The detailed workpiece setup and drilling sequence are shown in Fig. 3.

Tool wear and delamination assessment were conducted using defect indicators during the CFRP drilling process up to the 200th hole, as shown in Fig. 4. Tool wear was measured using a laser confocal microscope (VK-X3000, Keyence) after drilling through the entire CFRP plate

Table 1
Material properties of CFRP.

Parameter	Value
Fiber content (%)	67
Volume fraction of fiber (%)	57
Young's modulus, E_1 (GPa)	138
Young's modulus, E_2, E_3 (GPa)	8.02
Shear strength, τ_1 (MPa)	89
Shear strength, τ_2 (MPa)	63
Poisson's ratio, υ_{13}	0.31

Table 2
Mechanical properties of the support plates.

	Foam	Cork	Rubber	Aluminum
Density (g/cm^3)	0.04	0.18	1.635	2.7
Flexural strength (MPa)	0.3106	0.4733	1.1574	299.71
Flexural modulus (MPa)	13.4479	6.5047	7.1475	68900
Compressive modulus (MPa)	371.8	193.3	454.1	68900

corresponding to every 50 holes. The tool wear was quantified by measuring the worn area on the tool's flank face as shown in Fig. 5 [41–43]. The microscope images were analyzed using the ImageJ software to calculate the wear area. Delamination is one of the most critical defects affecting the hole quality. Delamination defects during drilling can occur at both the inlet and outlet, with the outlet being typically more severe [44]. This is due to the multilayered structure of the CFRP, where the layers tend to separate more as the drill bit exits the material. In this experiment, the delamination at the outlet was measured using a confocal microscope (VHX-7000, Keyence) at × 30 magnification. The delamination factor was calculated for quantitative analysis. Python 2.7 was used to implement an image-processing algorithm, and the process is illustrated in Fig. 6. An image of the drilled hole is shown in Fig. 6(a), and the center of the hole (green dot) is shown in Fig. 6(b). In Fig. 6(c), the contour (green line) of the delamination zone is shown. In Fig. 6(d), the delamination area, A_{del}, and nominal area (red circle), A_{nom}, were calculated to derive the delamination factor, F_a, using the following formula [45–47].

$$F_a = \frac{A_{del}}{A_{nom}} \tag{1}$$

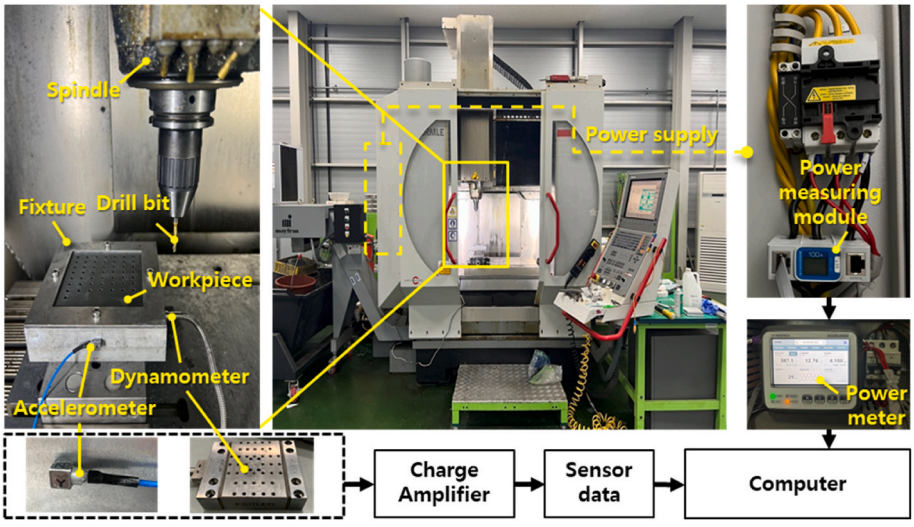

Fig. 2. Experimental setup for the CFRP drilling process.

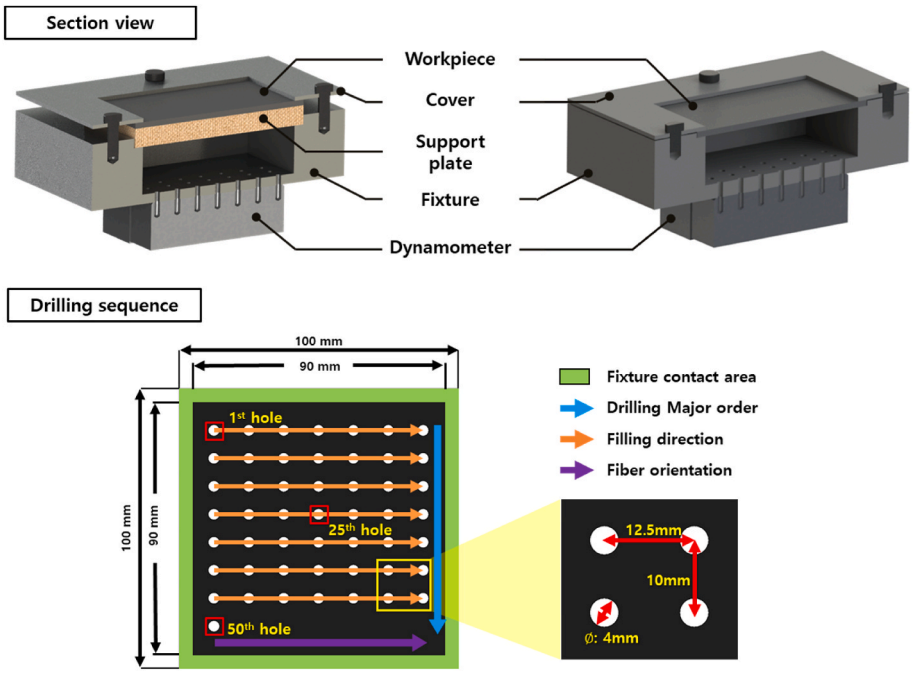

Fig. 3. Detailed workpiece setup and drilling sequence.

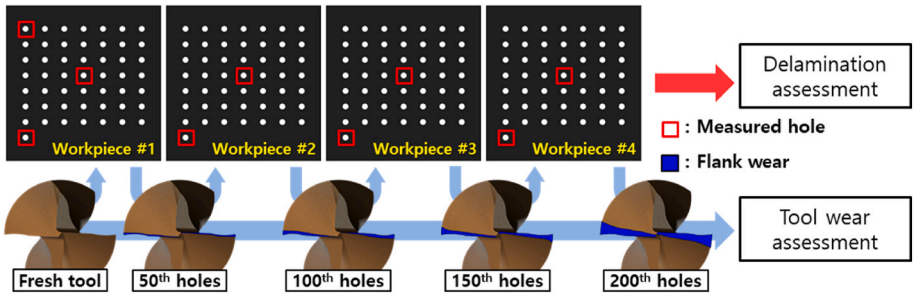

Fig. 4. Process up to the 200th hole for tool wear and delamination assessment in CFRP drilling.

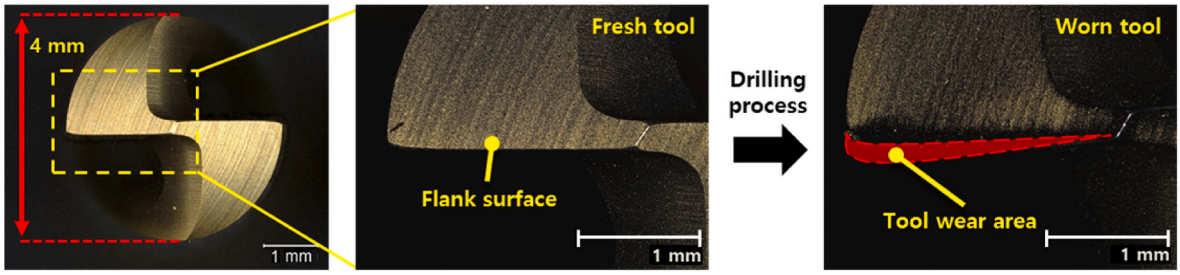

Fig. 5. Tool wear assessment for the drilling the CFRP.

3. Results and discussion

3.1. Thrust force

In CFRP drilling, the thrust force is a critical factor because it directly affects the tool wear, quality of the drilled holes, and overall structural integrity of the workpiece. The force profile in CFRP drilling differs between the cases with and without a support plate, primarily because of the differences in the cutting mechanism. As shown in Fig. 7(a), the drilling process using a support plate can be divided into five stages. Stage 1 begins when the chisel edge of the drill bit engages with the CFRP, making contact with only the chisel edge. In Stage 2, both the chisel edge and cutting lips of the tool cut into the workpiece, causing the thrust force to increase rapidly as the contact area increases. Stage 3 follows as the drill penetrates deeper into the CFRP, and the material starts to soften owing to rising temperatures, resulting in a gradual decrease in the thrust force. In Stage 4, the drill simultaneously cuts through both the CFRP and support plate, and the thrust force in this stage is largely influenced by the mechanical properties of the support plate. Finally, Stage 5 involves drilling only the support plate, where the cutting forces depend solely on the characteristics of the support plate. In contrast, drilling CFRP alone consists of Stages 1–4, without Stage 5.

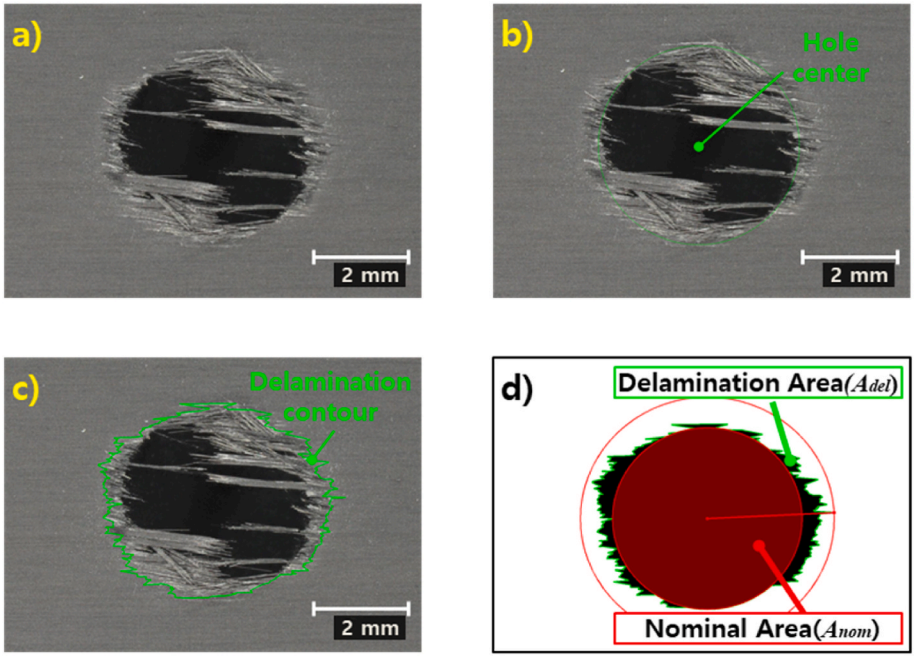

Fig. 6. Delamination assessment of a CFRP hole after the drilling process: (a) cropped image, (b) hole center, (c) delamination contour, and (d) delamination factor.

As shown in Fig. 7(b)–(f), the maximum thrust force typically occurs during the transition from Stages 2–3, regardless of whether a support plate is used. Fig. 8 presents an analysis of the maximum thrust force at intervals of 50 holes. The results indicated that the maximum thrust force tended to increase as the drilling process progressed, which was attributed to an increase in the tool wear. This wear expands the contact area between the tool and material, resulting in greater friction and higher cutting forces. Without a support plate, the workpiece experiences deflection due to the applied load from the drill, and when the drill breaks through the material, the deflection recovers, releasing stored energy and leading to sudden material failure. By using a support plate, the thrust force trend changes compared to drilling without one [48]. The effects of different support plate materials on the thrust force varied owing to the differences in their mechanical properties. Support plates with high stiffness generated greater counterforces, leading to an increased thrust force. However, those with high compressibility and excellent damping properties reduced deflection more effectively by absorbing vibrations during the drilling process, rather than merely resisting deformation. For instance, rigid materials such as aluminum generate a higher counterforce when drilling pressure is applied, leading to a higher thrust force. Conversely, porous materials such as foam and cork exhibit high compressibility, whereas rubber effectively dissipates energy to dampen vibrations and impact during drilling and reduce the thrust force.

3.2. Tool wear

Fig. 9 shows the tool wear under different support plate conditions during the drilling process. As observed from these images, no significant differences were present in the overall wear patterns between the different conditions. However, in the case of the aluminum-support plate, a prominent built-up edge was observed, where aluminum adhered to the tool owing to the high cutting forces, thereby accelerating tool wear. Fig. 10 provides a quantitative comparison of the tool wear area across different support plate conditions measured at 50-hole intervals. The results showed that tool wear consistently increased under all conditions, with the aluminum support plate exhibiting the highest wear. This is likely due to the increased cutting forces and higher rigidity of aluminum, which lead to greater counterforces on the tool. However, the rubber and cork support plates, which have good shock absorption properties, resulted in comparatively lower tool wear. These findings suggest that the material properties of the support plates influence the cutting forces exerted on the tool, thereby affecting the progression of tool wear.

3.3. Damping effect

Wavelet analysis was used to evaluate the vibrations that occurred during the drilling process with different support plates using the Morlet function in MATLAB, as shown in Fig. 11. A significant amplitude was observed at approximately 300 Hz, which corresponded to the main excitation frequency during the drilling process. Compared to drilling using only CFRP, the use of support plates such as foam, cork, and rubber showed a noticeable vibration-damping effect. These materials have a low elastic modulus, which allows them to absorb shocks and dissipate energy effectively, thereby reducing vibrations. By contrast, the aluminum support plate exhibited higher vibration amplitudes owing to its high stiffness, which caused it to transmit stresses rather than absorb them. In the latter part of the drilling process (from 1.5 to 2 s), as the tool began cutting through the support plate, the vibrations tended to increase. In the case of drilling with only CFRP (Fig. 11(a)), no significant increase in vibration was observed during this period. However, for the foam support plates (Fig. 11(b)), additional vibrations occurred, likely owing to the compression and expansion of the material during the process. For the cork support place (Fig. 11(c)), the vibrations increased when the cork was cut and torn during drilling. The rubber support plate (Fig. 11(d)) demonstrated relatively lower vibrations, which could be attributed to rubber softening or deformation due to the heat generated during drilling, allowing the rubber to absorb energy. In contrast, the aluminum support plate (Fig. 11(e)) exhibited higher vibrations caused by chip formation and the high stiffness of the material, which likely transmitted the stress rather than absorbing it. These observations indicated that the mechanical properties of the support plates significantly influenced the vibration patterns during drilling.

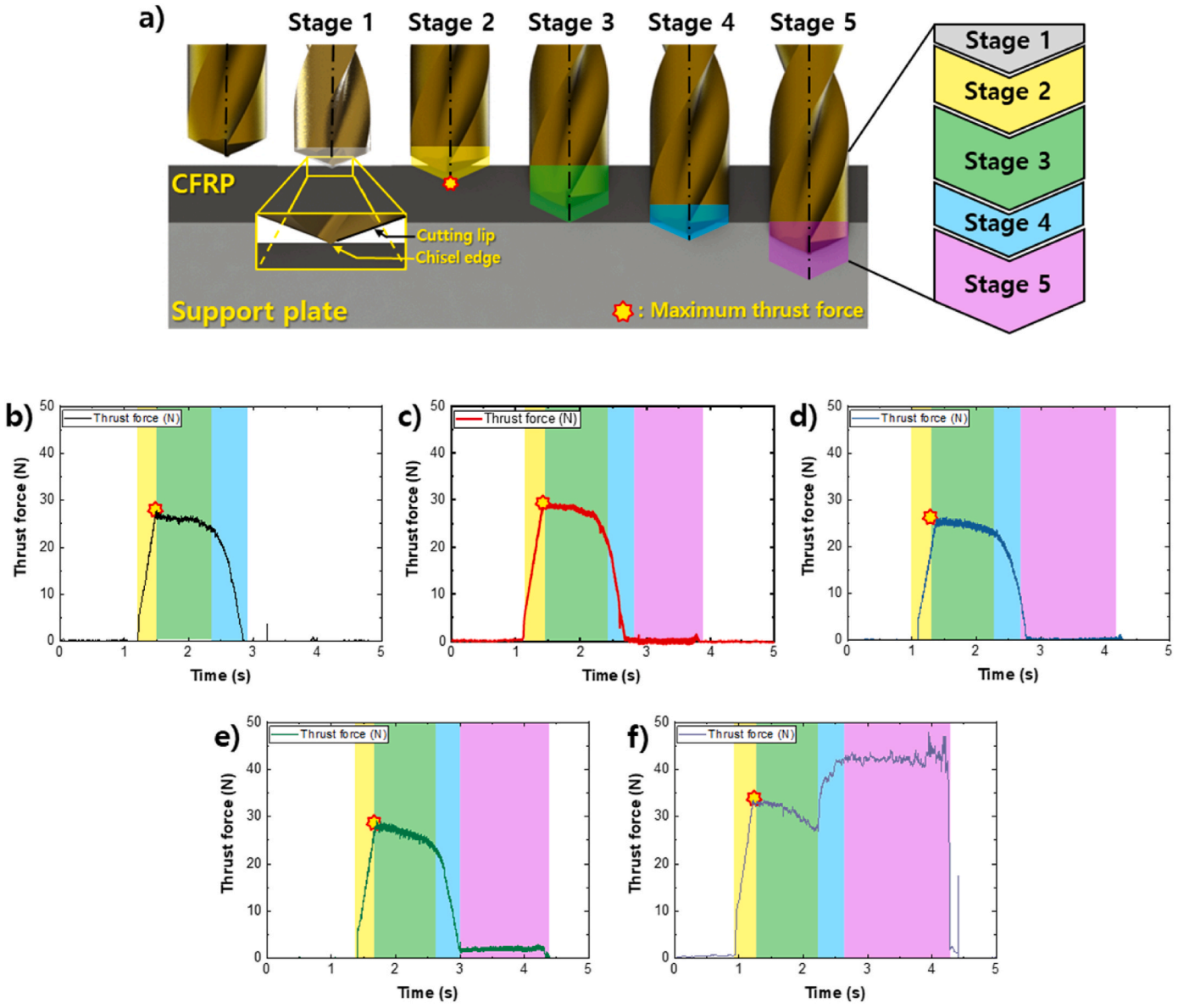

Fig. 7. (a) Schematic of the CFRP drilling process using different support plates and thrust forces at the first hole. Drilling process results for (b) CFRP only, (c) foam-stacked CFRP, (d) cork-stacked CFRP, (e) rubber-stacked CFRP, and (f) aluminum-stacked CFRP.

3.4. Delamination

The delamination evaluation was carried out using a microscope following the procedural steps outlined in Section 2. Fig. 12 illustrates how the extent of delamination varied based on the type of support plate used after drilling 200 holes. The hole image in Fig. 12(a) clearly indicates that the condition without a support plate exhibited the most severe delamination. When foam was used as the support plate (Fig. 12 (b)), there was a slight reduction in delamination, but significant defects were still evident. In contrast, using aluminum and rubber as support plates (Fig. 12(d) and (e)) resulted in much lower levels of delamination, demonstrating their effectiveness in mitigating defects. As shown in Fig. 13, the delamination factor was measured for every 25 holes starting from the first hole. The initial delamination factors for each condition were CFRP = 1.152, stacked foam = 1.140, stacked cork = 1.135, stacked rubber = 1.105, and stacked aluminum = 1.095, indicating a reduction in the initial delamination factor with the use of support plates. As drilling progressed, the delamination factor gradually increased, primarily because of the increase in the thrust force caused by tool wear. The highest delamination factor was observed at the 25th hole, which is attributed to the position of the hole within the specimen. As the hole approaches the central region, increased deflection occurs due to the geometric characteristics of the specimen and the corresponding boundary conditions of the support [44]. This leads to variations in stress distribution and thrust forces, which ultimately result in a greater susceptibility to delamination. Delamination tends to occur when deformation builds up, and the 25th hole, located closer to the center of the specimen, experienced the most significant deflection. For the 200th hole, the delamination factor decreased by 7.46% for the foam-stacked condition, 11.07% for the cork-stacked condition, and 12.45% for the rubber-stacked condition, compared to the CFRP-only condition. In contrast, the aluminum-stacked condition exhibited an increase of 17.59%. A delamination factor exceeding 1.2 is generally considered to indicate damage, and each support plate condition reached this threshold at different points, demonstrating varying levels of resistance to damage [49]. Delamination can be reduced by minimizing the deflection of the workpiece during drilling [50]. The thrust force applied during drilling can be considered as a concentrated load,

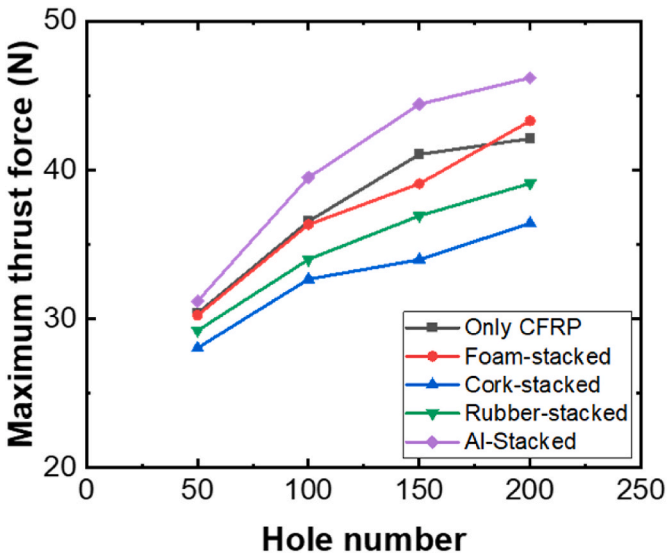

Fig. 8. Maximum thrust force for different support plate types after drilling each workpiece.

and its effect on the workpiece can be modeled using a simple beam deflection equation:

$$\delta_{max} = \frac{PL^3}{48 E_{eff} I_{eff}} \tag{2}$$

where the maximum deflection, δ_{max}, is inversely related to the effective moment of inertia, I_{eff}, and the effective Young's modulus, E_{eff}. The moment of inertia depends significantly on the thickness, which is calculated as

$$I_{eff} = \frac{b{t_{CFRP}}^3}{12} + \frac{b{t_{sup}}^3}{12} \tag{3}$$

where b represents the width, while t_{CFRP} and t_{sup} denote the thickness of the CFRP and support plate, respectively. When a support plate was applied, the overall thickness increased, leading to a higher effective moment of inertia and a reduced deflection. If the structure consisting of the CFRP and support plate is considered a laminated structure comprising two layers, the effective Young's modulus can be calculated using the weighted average of the modulus and thicknesses of the individual layers [51,52]:

$$E_{eff} = \frac{E_{CFRP} \bullet h_{CFRP} + E_{sup} \bullet h_{sup}}{\mathrm{h}} \tag{4}$$

where E_{CFRP} and E_{sup} are the Young's modulus of the CFRP and support plate, respectively, and h_{CFRP} and h_{sup} are their respective thicknesses. In this analysis, E_{CFRP} was taken E_1 (138 GPa), as provided in Table 1, representing the modulus along the fiber direction. Therefore, for support plates with the same total thickness, a higher effective Young's modulus led to a reduced deflection, making the combined structure more effective in minimizing delamination. This theoretical relationship illustrates that the aluminum support plate significantly reduces deflection compared to CFRP alone, achieving a reduction of approximately 91.5%. This substantial decrease can be attributed to the high flexural rigidity conferred by the combination of aluminum's thickness and modulus of elasticity. In contrast, other support materials such as foam, cork, and rubber demonstrate deflection reductions of approximately 77%, which are comparatively less pronounced. The findings suggest that, while deflection reduction is a critical factor in enhancing the drilling process, it may not be the sole determinant in mitigating defects such as delamination.

Initially, the aluminum-stacked condition showed the lowest delamination factor; however, as drilling progressed to the 200th hole, it exhibited a higher delamination factor than the rubber- and cork-stacked conditions. This change is associated with tool wear, as drilling with aluminum leads to faster tool degradation, resulting in an increased thrust force and a higher rate of delamination as more holes are drilled. The damping effect may also have influenced delamination, as materials such as cork and foam, which demonstrated lower vibration amplitudes at the excitation frequency, were able to effectively reduce delamination. Although rubber exhibited a comparatively lower vibration-damping capability, its higher compressive and flexural modulus provided a counteracting force to the thrust during drilling, allowing it to support the workpiece more effectively, resulting in the lowest overall delamination factor. The results of this study emphasize the importance of support plates in improving the drilling performance of CFRP. By reducing delamination and enhancing stability, support plates made of materials such as rubber, cork, and foam show significant potential for improving machining quality, especially in applications where minimizing defects is critical. While aluminum offers excellent deflection reduction due to its rigidity, its impact on tool wear underscores the importance of selecting materials that align with process sustainability goals. These findings provide valuable insights for optimizing CFRP drilling processes, suggesting that careful material selection can help balance defect reduction with tool longevity and

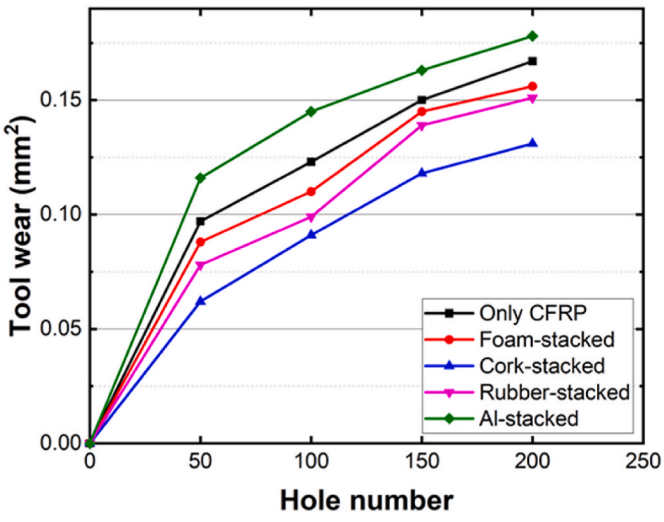

Fig. 10. Tool wear area for different support plate types after drilling each workpiece.

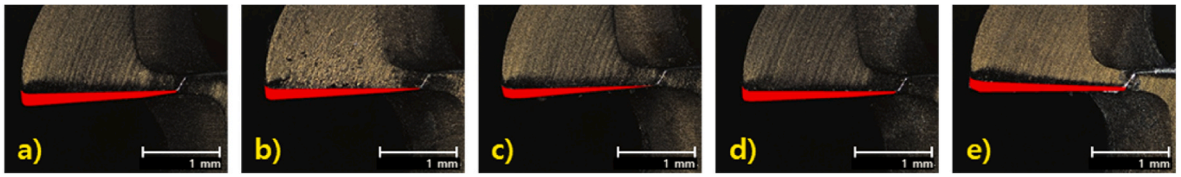

Fig. 9. Tool wear after drilling processes for 200 holes in different support plate types: (a) CFRP only, (b) foam-stacked CFRP, (c) cork-stacked CFRP, (d) rubber-stacked CFRP, and (e) aluminum-stacked CFRP.

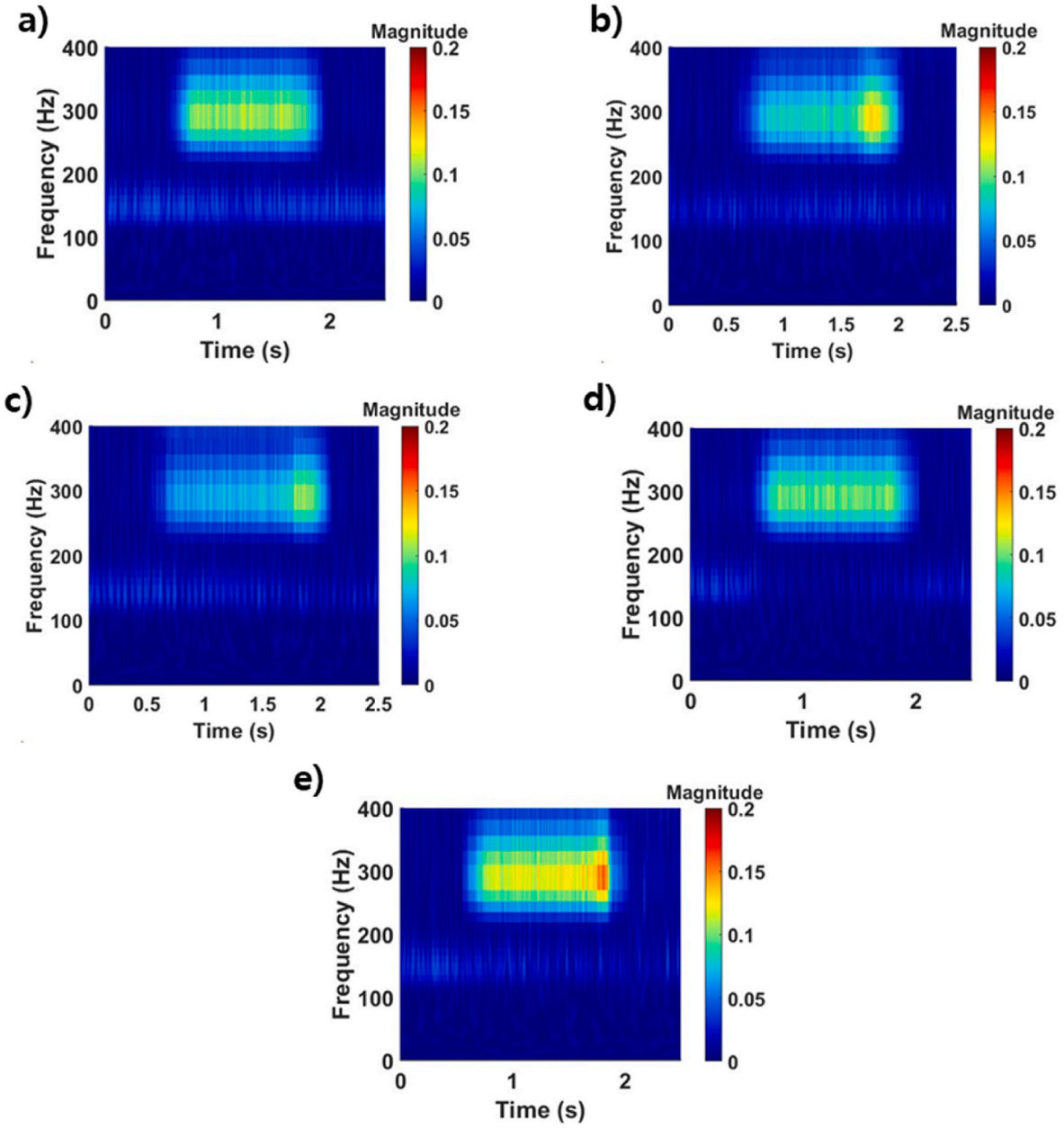

Fig. 11. Wavelet analysis of the vibration magnitude during the drilling process using different types of support plates: (a) CFRP only, (b) foam-stacked CFRP, (c) cork-stacked CFRP;,(d) rubber-stacked CFRP, and (e) aluminum-stacked CFRP.

operational efficiency.

3.5. Energy consumption

Fig. 14 shows the power consumption measured during the drilling of the first 50 holes in the CFRP. When the equipment was in the standby mode, the base power consumption was approximately 2.3 kW, and during drilling, it increased to a maximum of approximately 4.3 kW. The profile indicates a slight increase in power of up to approximately 3.4 kW during the drilling phase, whereas a significant spike in power consumption occurred when the spindle moved between the hole-machining operations. The area under the power curve represents the total energy consumption and was used to calculate the total energy consumed during the drilling process with different support plates. Fig. 15 shows the accumulated energy consumption for drilling 200 holes under each condition. The energy consumptions for each condition were as follows: 0.9896 kWh for CFRP, 0.9887 kWh for foam stacking, 0.9871 kWh for cork stacking, 0.9858 kWh for rubber stacking, and 0.9982 kWh for aluminum stacking. The variations in energy consumption across different support plate conditions were relatively small. This is primarily because the energy consumed during the cutting operations is less significant than the energy required when the spindle travels between the holes. Most of the energy consumption was associated with maintaining the base power during the drilling process, which minimized the differences in power usage between the different support plate conditions.

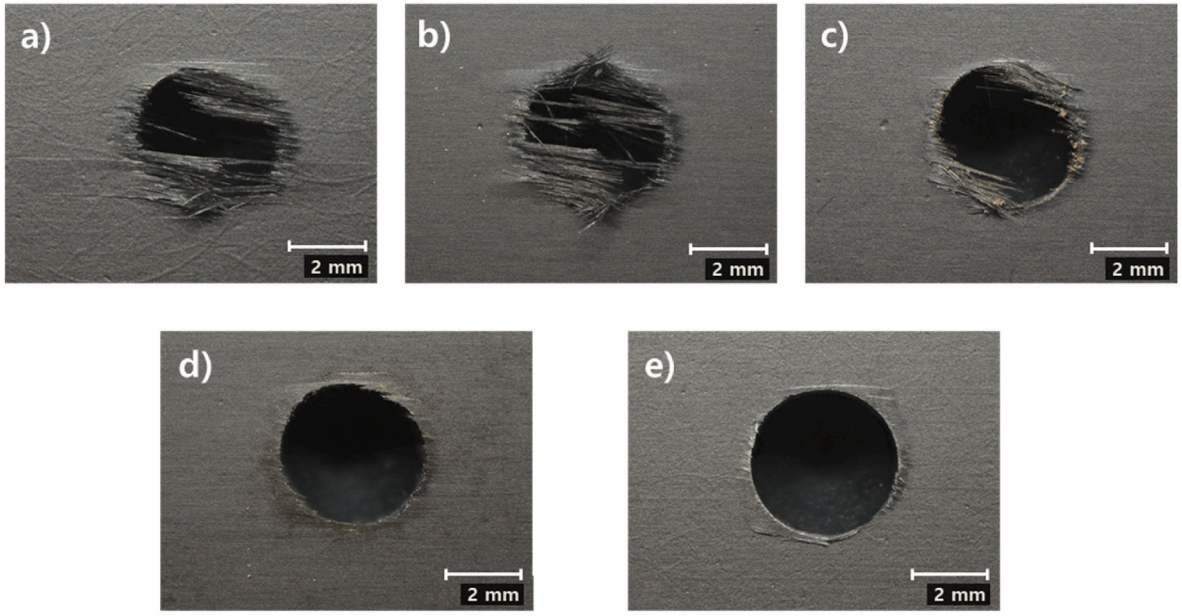

Fig. 12. Delamination of the outlet hole after drilling 200 holes: (a) CFRP only, (b) foam-stacked CFRP, (c) cork-stacked CFRP, (d) rubber-stacked CFRP, and (e) aluminum-stacked CFRP.

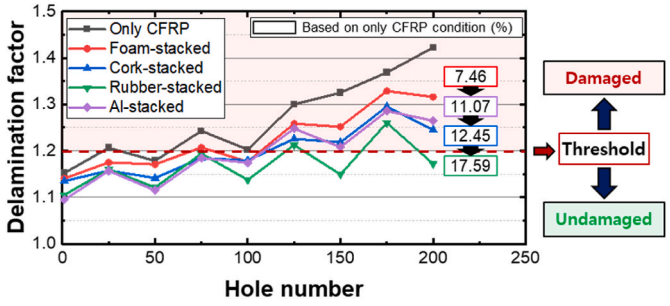

Fig. 13. Delamination factor at the selected holes for all workpiece types: CFRP only (black, squares), foam-stacked CFRP (red, circles), cork-stacked CFRP (blue, triangles), rubber-stacked CFRP (green, inverted triangles), and aluminum-stacked CFRP (purple, diamonds).

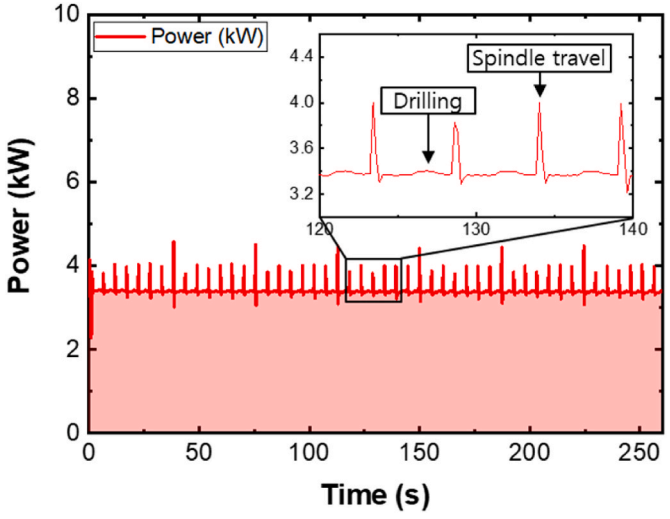

Fig. 14. Power of the CFRP drilling process for the workpiece.

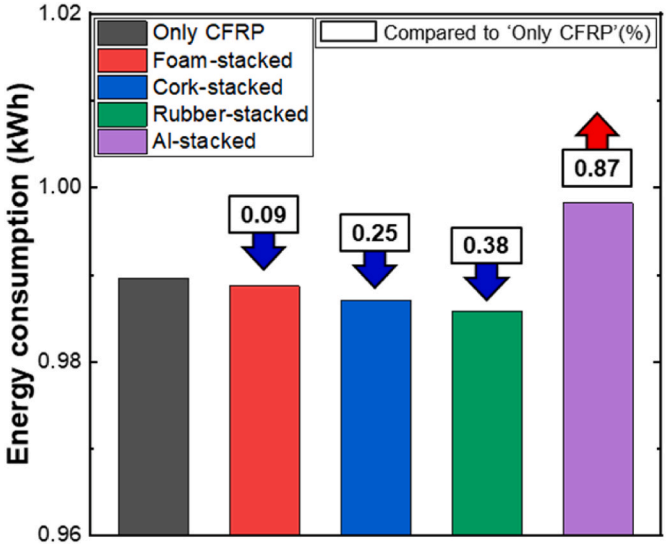

Fig. 15. Energy consumption during the drilling of 200 holes.

4. Sustainability assessment

CFRP requires strict tolerances, indicating the need for a model that evaluates economic efficiency and determines quality standards based on defects that occur during the drilling process. This study proposes a machining economics model based on defects incurred during the CFRP drilling process to assess its economic efficiency. The model includes various factors, such as material cost, tooling cost, energy consumption, and setup cost. This model is designed to maintain quality by setting a threshold for the delamination factor, and the tool is replaced to ensure that quality standards are met when this threshold is reached.

4.1. Economic analysis

4.1.1. Cost of workpiece

The dimensions of the CFRP specimen were 100 × 100 × 3 mm, and those of the support plate were 100 × 100 × 10 mm. The individual costs

Table 3
Workpiece costs.

Material	CFRP	Foam	Cork	Rubber	Aluminum
Unit cost (USD)	72	4	8	18	45
Machining condition	Only CFRP	Foam-stacked	Cork-stacked	Rubber-stacked	Aluminum-stacked
Cost per workpiece (USD)	72	76	80	90	117
Total cost of workpieces, C_w (USD)	288	304	320	360	468

of the CFRP and support plates made of various materials were determined based on their purchase prices. Unlike the CFRP condition, the condition of using a support plate includes the additional cost of the support plate along with the CFRP. The total workpiece cost, C_w, was calculated based on the requirement of four plates to machine 200 holes, as investigated in the experiment as following equation:

$$C_w = 4 \times \left(C_{CFRP} + C_{support}\right) \tag{5}$$

where C_{CFRP} and $C_{support}$ represent the unit costs of the CFRP and support plate specimens, respectively. A cost comparison of the workpieces under each experimental condition is presented in Table 3.

4.1.2. Cost of tooling

The tooling cost represents the expenses associated with tool wear and replacement owing to degradation during the drilling process. In this study, the threshold for delamination was set to 1.2, meaning that the tools were replaced when the delamination factor reached or exceeded this limit to ensure that the quality standards were maintained. The threshold was determined experimentally based on the increase in the delamination factor from the initial level to the threshold level. For each support plate condition, the tooling cost per 200 holes was calculated by dividing the total number of holes by the effective lifespan of the tool under each condition, denoted as TH, which represents the number of holes that the tool could drill before reaching the delamination threshold. The equation used to calculate the tool lifespan under these conditions is:

$$TH = \frac{F_{a,threshold} - F_{a,initial}}{\Delta F_a / N} \tag{6}$$

where $F_{a,threshold}$ is the delamination factor threshold, $F_{a,initial}$ is the delamination factor of the first hole, ΔF_a represents the incremental change per hole, and N is the number of drilled holes. Then, cutting tool cost, C_t, for drilling 200 holes is derived as following:

$$C_t = T_u \times \frac{200}{TH} \tag{7}$$

Where T_u represents the tool cost per unit and the second term represents the required number of tools for drilling 200 holes. The resulting tooling costs for each support plate are listed in Table 4.

Table 4
Tooling costs for the CFRP drilling process.

	Only CFRP	Foam-stacked	Cork-stacked	Rubber-stacked	Aluminum-stacked
Tool cost per unit (USD)	40	40	40	40	40
TH	47.81	72.71	102.57	175.00	108.79
Required tools for 200 holes	4.18	2.75	1.95	1.14	1.84
Cutting tool cost (USD)	167.32	110.03	77.99	45.71	73.54

4.1.3. Cost of labor

Labor costs arise from various stages of the machining process, including setup, tool changing, and machining, and the total labor cost is the sum of these components. The labor cost for setup, $C_{l,setup}$, was calculated by multiplying the setup time, number of setups required per workpiece, and the labor rate, L_r. The setup time, t_{setup}, was longer when a support plate was used because additional time was required to attach the support plate beneath the CFRP. The labor cost for tool-changing, $C_{l,tool\text{-}changing}$, was determined by the time required for each tool change, the number of tools required to machine 200 holes, and the labor rate. The frequency of tool changes varied depending on the type of support plate used because different support plates affect the extent of defects and determine the number of holes that can be machined before reaching the threshold. The labor cost for machining, $C_{l,machining}$, was calculated by multiplying the machining time by the labor rate, and the machining time was consistent across all conditions. The equations for the components contributing to labor cost are as follows:

$$C_{l,setup} = L_r \times t_{setup} \times N_s \tag{8}$$

$$C_{l,tool-changing} = L_r \times t_{tool-chaning} \times \frac{200\ holes}{TH} \tag{9}$$

$$C_{l,machining} = L_r \times t_m \tag{10}$$

$$C_l = C_{l,setup} + C_{l,tool-changing} + C_{l,machining} \tag{11}$$

The detailed information from above equations is summarized in Table 5.

4.1.4. Energy consumption

Energy consumption occurs throughout all the stages of the process. During the setup stage, the idle power, P_I, from the equipment was consumed, and the energy consumption for setup, $E_{c,setup}$, was calculated as Eq. (12). Similarly, in the tooling stage, idle power is consumed while changing tools; therefore, the energy consumption for tool-changing, $E_{c,tool\text{-}changing}$, was determined as Eq. (13).

$$E_{c,setup} = P_I \times t_{setup} \tag{12}$$

$$E_{c,tool-changing} = P_I \times t_{tool-changing} \times \text{Required tools for 200 holes} \tag{13}$$

During CFRP drilling, the power output of the equipment varies depending on the support plate conditions. The energy consumption cost was obtained by multiplying the total energy consumption of all the processes by the energy cost, which was set at 0.22 USD/kWh [53].

$$C_e = energy\ cost \times \left(E_{c,setup} + E_{c,tool-changing} + E_{c,machining}\right) \tag{14}$$

The details of the calculations for each stage are presented in Table 6.

4.1.5. Overall cost

In the CFRP drilling process using support plates, the total cost for each condition was determined as the sum of the workpiece, tooling, labor, and energy consumption costs, as shown in the following equation:

$$C_{total} = C_w + C_t + C_l + C_e \tag{15}$$

The cost per hole for each condition was calculated by dividing the overall cost by the total number of holes drilled, as shown in Table 7. The ratio based on only CFRP represents the relative cost of each condition compared to the CFRP-only baseline. For example, the rubber-stacked condition, which amounted to 89.13% of the baseline cost, showed an extended tool life owing to its excellent vibration-damping properties, resulting in lower tool change costs. In contrast, the aluminum-stacked condition showed fewer delamination defects but was economically less favorable, with a cost ratio of 118.69% owing to the high expense of the workpiece material. The cork-stacked condition proved to be the most cost-effective support plate material, with an

Table 5
Labor costs for the CFRP drilling process.

		Only CFRP	Foam-stacked	Cork-stacked	Rubber-stacked	Aluminum-stacked
Setup	Setup time, t_{setup} (s)	180	240	240	240	240
	Labor rate, L_r (USD/h)	9.812	9.812	9.812	9.812	9.812
	Number of pieces made for the setup, N	4	4	4	4	4
	Labor cost, $C_{l,setup}$ (USD)	1.96	2.62	2.62	2.62	2.62
Tool changing	Tool changing time, $t_{tool\text{-}chaning}$ (s)	200	200	200	200	200
	Required tools for 200 holes	4.183	2.751	1.950	1.143	1.838
	Labor rate, L_r (USD/h)	9.812	9.812	9.812	9.812	9.812
	Labor cost, $C_{l,tool\text{-}changing}$ (USD)	2.280	1.50	1.06	0.62	1.00
Machining	Machining time, t_m (s)	260	260	260	260	260
	Labor rate, L_r (USD/h)	9.812	9.812	9.812	9.812	9.812
	Labor cost, $C_{l,machining}$ (USD)	0.709	0.709	0.709	0.709	0.709
Total	Labor cost (USD)	4.951	4.825	4.388	3.948	4.327

Table 6
Energy consumption for the CFRP drilling process.

		Only CFRP	Foam-stacked	Cork-stacked	Rubber-stacked	Aluminum-stacked
Setup	Idle power, P_I (kW)	2.3	2.3	2.3	2.3	2.3
	Setup time, t_{setup} (s)	180	240	240	240	240
	Energy consumption, $E_{c,setup}$ (kWh)	0.460	0.613	0.613	0.613	0.613
	Energy consumption cost (USD)	0.101	0.135	0.135	0.135	0.135
Tooling	Idle power, P_I (kW)	2.3	2.3	2.3	2.3	2.3
	Tool changing time, $t_{tool\text{-}chaning}$ (s)	200	200	200	200	200
	Required tools for 200 holes	4.183	2.751	1.950	1.143	1.838
	Energy consumption, $E_{c,tool\text{-}changing}$ (kWh)	0.534	0.351	0.249	0.146	0.235
	Energy consumption cost (USD)	0.118	0.077	0.055	0.032	0.052
Machining	Energy consumption, $E_{c,machining}$ (kWh)	0.990	0.989	0.987	0.986	0.998
	Energy consumption cost (USD)	0.218	0.217	0.217	0.217	0.220
Total	Energy consumption, C_e (USD)	0.437	0.430	0.407	0.384	0.406

Table 7
Overall costs of the CFRP drilling process.

	Only CFRP	Foam-stacked	Cork-stacked	Rubber-stacked	Aluminum-stacked
Total cost for 200 holes (USD)	460.71	419.28	402.79	410.05	546.27
Total cost per 1 hole (USD)	2.30	2.09	2.01	2.05	2.73
Ratio based on only CFRP (%)	100.00	90.87	87.39	89.13	118.69

overall cost of 87.39% compared to CFRP alone. This is attributed to the ability of cork to enhance the machining stability while maintaining a reasonable material cost. Cork is a renewable and biodegradable material that can be harvested in an eco-friendly manner, making it particularly suitable as a support plate for environmentally friendly and sustainable drilling processes.

4.1.6. *Threshold effect on costs*

In the machining cost analysis, a delamination factor threshold of 1.2 was used; however, this threshold can vary depending on the quality requirements [44]. Fig. 16 illustrates the cost per hole during CFRP drilling for each support plate type when 200 holes were processed with varying delamination factor thresholds. As the threshold increases, the cost per hole generally decreases under all conditions. This occurred because the machining conditions and time remained consistent, indicating that the material and setup costs were fixed. However, with a

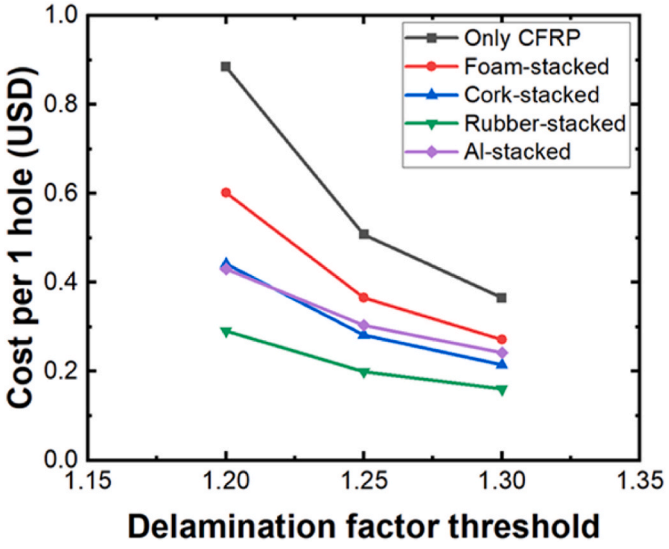

Fig. 16. Effect of the delamination threshold on the cost per hole in CFRP drilling using different support plates.

Table 8
CO_2 emission of the support plates.

	Foam	Cork	Rubber	Aluminum
CO_2 emission (kg)	3.01 [54]	0.81 [55]	3.40 [56]	4.00 [56]
Energy consumption (MJ/kg)	86.4 [54]	4.0 [55]	40.3 [56]	45.8 [56]

higher threshold, each tool can process more holes before reaching its limit, thereby reducing the tool replacement frequency. This reduction in tool replacement leads to lower tooling costs because fewer tools are consumed over the same number of holes. Additionally, fewer tool changes contribute to a more efficient process, minimizing downtime and associated labor costs and further enhancing cost efficiency. This demonstrates that adjusting the set threshold allows the model to meet various quality requirements and efficiently manage the overall machining costs.

4.2. CO_2 emission

Based on the data presented in Table 8, which compares the CO_2 emissions and energy consumption of materials selected as support plates in CFRP drilling, the following conclusions can be drawn. Here, energy consumption refers to the energy required for the production of the materials. Rubber and Aluminum support plates record CO_2 emissions of 3.40 kg and 4.00 kg, respectively, with energy consumption of 40.3 MJ/kg and 45.8 MJ/kg, indicating higher environmental impacts compared to Cork. Although Foam support plates are cost-effective, they exhibit a relatively high CO_2 emission of 3.01 kg and the highest energy consumption of 86.4 MJ/kg, raising significant environmental concerns. In contrast, Cork support plates, with the lowest CO_2 emission of 0.81 kg and the lowest energy consumption of 4.0 MJ/kg, are considered the most suitable option when prioritizing environmental sustainability and energy efficiency.

5. Conclusion

The increasing use of CFRPs in aerospace applications demands high manufacturing quality while maintaining economic efficiency. Although support plate methods have been proposed to reduce drilling defects, their economic viability has not been thoroughly investigated, especially considering the strict quality requirements for aerospace components. This study conducted a comprehensive analysis of various support plate materials (foam, rubber, cork, and aluminum) in CFRP drilling, examining the thrust force, tool wear, damping effects, delamination, and energy consumption. A machining economics model was also proposed that incorporates quality thresholds. The following main conclusions were drawn.

1. Distinct thrust force characteristics were analyzed in stages with and without support plates, and the maximum thrust forces were compared between the conditions. The analysis showed that rigid materials, such as aluminum, generated higher counterforces, whereas porous and flexible materials (foam, cork, and rubber) reduced the thrust forces through their damping properties.
2. Tool wear was quantitatively evaluated by measuring the tool wear area at 50-hole intervals. Although the tool wear area increased with the number of drilled holes under all conditions, there were no significant differences in the wear progression between the different support plate conditions. The results showed a general increasing trend in the tool wear area, regardless of the support plate material that was used.
3. Wavelet analysis of the vibrations identified significant amplitudes at approximately 300 Hz during CFRP drilling. Foam, cork, and rubber demonstrated effective vibration damping through reduced amplitudes in this frequency range compared with unsupported drilling. In contrast, the high stiffness of aluminum resulted in increased vibration transmission, particularly in the latter stages of drilling, owing to its inability to absorb and dissipate cutting energy effectively.
4. Delamination analysis revealed varying degrees of defect reduction. Cork and rubber support plates achieved 11.07% and 12.45% reductions in the delamination factor, respectively, after 200 holes, whereas aluminum showed a 17.59% increase compared to unsupported drilling. This effectiveness is attributed to the combined effect of the increased moment of inertia and appropriate material stiffness.
5. The machining economics model, incorporating a delamination factor threshold of 1.2, revealed significant cost variations under different support conditions. Cork-stacked drilling demonstrated the highest economic efficiency, reducing overall costs by 12.6% compared with unsupported drilling, whereas aluminum increased costs by 18.6%.
6. In terms of CO_2 emissions, Cork stands out as the most environmentally friendly support plate material, with an emission level of 0.807 kg.

Considering both the experimental defect reduction performance and sustainable assessment results, cork emerged as the most cost-effective support plate material, offering an optimal balance between machining quality and economic efficiency, and reduced CO_2 emissions while providing additional benefits of environmental sustainability through its renewable and biodegradable nature. Future research could explore cork's performance under diverse machining conditions and its applicability to complex geometries, such as curved surfaces, to validate its use in real aerospace components. These findings demonstrate cork's potential for sustainable manufacturing, aligning with industry trends toward defect suppression and carbon neutrality.

CRediT authorship contribution statement

Yun Seok Kang: Writing – original draft, Visualization, Methodology, Formal analysis, Data curation. **Dong Eun Kim:** Validation, Software, Investigation. **Hyung Wook Park:** Supervision, Resources, Project administration. **Jaewoo Seo:** Writing – review & editing, Supervision, Conceptualization.

Declaration of competing interest

The authors declare the following financial interests/personal relationships which may be considered as potential competing interests: Hyung Wook Park reports financial support was provided by Korea Ministry of Science and ICT. Hyung Wook Park reports financial support was provided by Korea Ministry of Trade Industry and Energy. If there are other authors, they declare that they have no known competing financial interests or personal relationships that could have appeared to influence the work reported in this paper.

Acknowledgements

This work was supported by the National Research Foundation of Korea (NRF) funded by the Ministry of Science and ICT of Korea (No. 2022R1A2C3007963), Development of smart manufacturing multiverse platform based on multisensory fusion avatar and interactive AI funded by the Ministry of Trade, Industry and Energy (20025702), and Development of generative Albased immersive metaverse factory technology through the Institute for Information and Communications Technology Promotion (IITP) funded by the Ministry of Science and ICT of Korea (No. RS-2024-00423300)

Nomenclature

MQL	minimum quantity lubrication
E_{eff}	effective Young's modulus
E_{CFRP}	Young's modulus of CFRP
E_{sup}	Young's modulus of support plate
t_{CFRP}	thickness of CFRP
t_{sup}	thickness of support plate
I_{eff}	effective moment of inertia
A_{del}	delamination area (mm^2)
A_{nom}	nominal area (mm^2)
F_a	delamination factor
TH	effective lifespan of the tool
$F_{a,threshold}$	delamination factor threshold
$F_{a,initial}$	delamination factor for 1st hole
ΔF_a	incremental change per hole
C_t	Cutting tool cost (USD)
T_u	unit cost of tool (USD)
$C_{l,setup}$	labor cost for setup (USD)
L_r	labor rate (USD/h)
t_{setup}	setup time (s)
N_s	the number of pieces made for the setup
$C_{l,tool\text{-}changing}$	labor cost for tool-changing (USD)
$t_{tool\text{-}changing}$	tool changing time (s)
$C_{l,machining}$	labor cost for machining (USD)
t_m	machining time (s)
$E_{c,setup}$	energy consumption of setup (kwh)
P_I	idle power of CNC machine (W)
$E_{c,tool\text{-}changing}$	energy consumption of tool-changing (kwh)
$E_{c,machining}$	energy consumption of machining (kwh)
C_e	energy consumption cost (USD)

Data availability

Data will be made available on request.

References

[1] R.S. Chandel, R. Kumar, J. Kapoor, Sustainability aspects of machining operations: a summary of concepts, Mater. Today Proc. 50 (2022) 716–727, https://doi.org/10.1016/j.matpr.2021.04.624.

[2] N. Khanna, et al., In pursuit of sustainability in machining thin walled α-titanium tubes: an industry supported study, Sustain. Mater. Technol. 36 (2023) e00647, https://doi.org/10.1016/j.susmat.2023.e00647.

[3] S. Ma, et al., Industry 4.0 and cleaner production: a comprehensive review of sustainable and intelligent manufacturing for energy-intensive manufacturing industries, J. Clean. Prod. (2024) 142879, https://doi.org/10.1016/j.jclepro.2024.142879.

[4] P. Shah, et al., Life cycle assessment to establish sustainable cutting fluid strategy for drilling Ti-6Al-4V, Sustain. Mater. Technol. 30 (2021) e00337, https://doi.org/10.1016/j.susmat.2021.e00337.

[5] B. Denkena, et al., Energy efficient machine tools, CIRP Annals 69 (2020) 646–667, https://doi.org/10.1016/j.cirp.2020.05.008.

[6] X. Yan, Y.-p. Fang, CO2 emissions and mitigation potential of the Chinese manufacturing industry, J. Clean. Prod. 103 (2015) 759–773, https://doi.org/10.1016/j.jclepro.2015.01.051.

[7] E. Akbostancı, G.İ. Tunç, S. Türüt-Aşık, CO2 emissions of Turkish manufacturing industry: a decomposition analysis, Appl. Energy 88 (2011) 2273–2278, https://doi.org/10.1016/j.apenergy.2010.12.076.

[8] N. Floros, A. Vlachou, Energy demand and energy-related CO2 emissions in Greek manufacturing: assessing the impact of a carbon tax, Energy Econ. 27 (2005) 387–413, https://doi.org/10.1016/j.eneco.2004.12.006.

[9] M.Y. Khalid, et al., Recent trends in recycling and reusing techniques of different plastic polymers and their composite materials, Sustain. Mater. Technol. 31 (2022) e00382, https://doi.org/10.1016/j.susmat.2021.e00382.

[10] L. Zhang, A. Sojobi, K. Liew, Sustainable CFRP-reinforced recycled concrete for cleaner eco-friendly construction, J. Clean. Prod. 233 (2019) 56–75, https://doi.org/10.1016/j.jclepro.2019.06.025.

[11] D. Liu, Y. Tang, W. Cong, A review of mechanical drilling for composite laminates, Compos. Struct. 94 (2012) 1265–1279, https://doi.org/10.1016/j.compstruct.2011.11.024.

[12] A. Al-Lami, P. Hilmer, M. Sinapius, Eco-efficiency assessment of manufacturing carbon fiber reinforced polymers (CFRP) in aerospace industry, Aero. Sci. Technol. 79 (2018) 669–678, https://doi.org/10.1016/j.ast.2018.06.020.

[13] S. Morkavuk, U. Köklü, K. Aslantaş, An experimental investigation on the influence of different surface curvatures in drilling machinability of carbon fiber reinforced plastic, Proc. Inst. Mech. Eng. Part C J. Mech. Eng. Sci. 236 (2022) 10953–10968, https://doi.org/10.1177/09544062221110466.

[14] D. Zhang, et al., Delamination in rotary ultrasonic machining of CFRP composites: finite element analysis and experimental implementation, Int. J. Adv. Manuf. Technol. 107 (2020) 3847–3858, https://doi.org/10.1007/s00170-020-05310-0.

[15] A. Abrao, et al., The effect of cutting tool geometry on thrust force and delamination when drilling glass fibre reinforced plastic composite, Mater. Des. 29 (2008) 508–513, https://doi.org/10.1016/j.matdes.2007.01.016.

[16] L. Kong, D. Gao, Y. Lu, Novel tool for damage reduction in orbital drilling of CFRP composites, Compos. Struct. 273 (2021) 114338, https://doi.org/10.1016/j.compstruct.2021.114338.

[17] Q. Wang, X. Jia, Optimization of cutting parameters for improving exit delamination, surface roughness, and production rate in drilling of CFRP composites, Int. J. Adv. Manuf. Technol. 117 (2021) 3487–3502, https://doi.org/10.1007/s00170-021-07918-2.

[18] Q. Wang, X. Jia, Optimization of cutting parameters for improving exit delamination, surface roughness, and production rate in drilling of CFRP composites, Int. J. Adv. Manuf. Technol. 117 (2021) 3487–3502, https://doi.org/10.1007/s00170-021-07918-2.

[19] A. Elhadi, et al., Evaluation of drilling by induced delamination of hybrid biocomposites reinforced with natural fibers: a statistical analysis by RSM, J. Compos. Mater. 58 (2024) 2515–2530, https://doi.org/10.1177/00219983241271035.

[20] J. Seo, et al., Recent developments and challenges on machining of carbon fiber reinforced polymer composite laminates, Int. J. Precis. Eng. Manuf. 22 (2021) 2027–2044, https://doi.org/10.1007/s12541-021-00596-w.

[21] F. Panella, A. Pirinu, Application of pulsed thermography and post-processing techniques for CFRP industrial components, J. Nondestruct. Eval. 40 (2021) 52, https://doi.org/10.1007/s10921-021-00776-8.

[22] Ç. Betgül, U. Köklü, S. Morkavuk, The effects of support plate thickness on the drilling machinability of CFRP, J. Reinforc. Plast. Compos. (2023) 07316844231218942, https://doi.org/10.1177/07316844231218942.

[23] C. Tsao, H. Hocheng, A review of backup mechanism for reducing delamination when drilling composite laminates J, Res. Updates Polym. Sci. 5 (2016) 97–107, https://doi.org/10.6000/1929-5995.2016.05.03.2.

[24] Ş. Yazman, et al., Investigation of the effect of symmetrical hybrid stacking on drilling machinability of unidirectional CFRP, GFRP and hybrid composites:

drilling tests and damage analysis, ompos. Part A Appl. Sci. Manuf. 187 (2024) 108486, https://doi.org/10.1016/j.compositesa.2024.108486.
[25] A. Dogrusadik, A. Kentli, Comparative assessment of support plates' influences on delamination damage in micro-drilling of CFRP laminates, Compos. Struct. 173 (2017) 156–167, https://doi.org/10.1016/j.compstruct.2017.04.031.
[26] Y.S. Kang, et al., Experimental investigation of simple foam-stacked in drilling process for carbon fiber reinforced plastic, J. Reinforc. Plast. Compos. (2023) 07316844231216808, https://doi.org/10.1177/07316844231216808.
[27] M.-C. Chen, Optimizing machining economics models of turning operations using the scatter search approach, Int. J. Prod. Res. 42 (2004) 2611–2625, https://doi.org/10.1080/00207540410001666251.
[28] Y.-C. Wang, et al., Optimization of machining economics and energy consumption in face milling operations, Int. J. Adv. Manuf. Technol. 99 (2018) 2093–2100, https://doi.org/10.1007/s00170-018-1848-6.
[29] P. Muthuswamy, An environment-friendly sustainable machining solution to reduce tool consumption and machining time in face milling using a novel wiper insert, Mater. Today Sustain. 22 (2023) 100400, https://doi.org/10.1016/j.mtsust.2023.100400.
[30] N. Makul, Modern sustainable cement and concrete composites: review of current status, challenges and guidelines, Sustain. Mater. Technol. 25 (2020) e00155, https://doi.org/10.1016/j.susmat.2020.e00155.
[31] Q. Wang, et al., A mechanics based prediction model for tool wear and power consumption in drilling operations and its applications, J. Clean. Prod. 234 (2019) 171–184, https://doi.org/10.1016/j.jclepro.2019.06.148.
[32] H.E. Yan, et al., Sustainability assessment during machining processes: evidence from the econ-environmental modelling, J. Clean. Prod. 448 (2024) 141612, https://doi.org/10.1016/j.jclepro.2024.141612.
[33] D.M. Kim, H.I. Kim, H.W. Park, Tool wear, economic costs, and CO2 emissions analysis in cryogenic assisted hard-turning process of AISI 52100 steel, Sustain. Mater. Technol. 30 (2021) e00349, https://doi.org/10.1016/j.susmat.2021.e00349.
[34] K.M. Hubbard, R.N. Callahan, S.D. Strong, A standardized model for the evaluation of machining coolant/lubricant costs, Int. J. Adv. Manuf. Technol. 36 (2008) 1–10, https://doi.org/10.1007/s00170-006-0806-x.
[35] T. Sivarupan, et al., A review of the use of cryogenic coolant during machining titanium alloys, Sustain. Mater. Technol. (2024) e00946, https://doi.org/10.1016/j.susmat.2024.e00946.
[36] Ç.V. Yıldırım, et al., Analysis of machinability and sustainability aspects while machining Hastelloy C4 under sustainable cutting conditions, Sustain. Mater. Technol. 38 (2023) e00781, https://doi.org/10.1016/j.susmat.2023.e00781.
[37] Z. Shi, et al., Sustainable and environmentally friendly longitudinal-torsional ultrasonic cryogenic cooling drilling system, J. Clean. Prod. 468 (2024) 143001, https://doi.org/10.1016/j.jclepro.2024.143001.
[38] A. Race, et al., Environmentally sustainable cooling strategies in milling of SA516: effects on surface integrity of dry, flood and MQL machining, J. Clean. Prod. 288 (2021) 125580, https://doi.org/10.1016/j.jclepro.2020.125580.
[39] J. Xu, et al., A critical review addressing drilling-induced damage of CFRP composites, Compos. Struct. 294 (2022) 115594, https://doi.org/10.1016/j.compstruct.2022.115594.
[40] W. Knapp, Trends and future possibilities of ISO standards for machine tools. Laser Metrol. Mach. Perform. X., 2013, 331-321.
[41] X. Yu, et al., Image edge detection based tool condition monitoring with morphological component analysis, ISA Trans. 69 (2017) 315–322, https://doi.org/10.1016/j.isatra.2017.03.024.
[42] J. Su, C. Huang, Y. Tarng, An automated flank wear measurement of microdrills using machine vision, J. Mater. Process. Technol. 180 (2006) 328–335, https://doi.org/10.1016/j.jmatprotec.2006.07.001.
[43] W. Wang, G.S. Hong, Y. Wong, Flank wear measurement by a threshold independent method with sub-pixel accuracy, Int. J. Mach. Tool Manufact. 46 (2006) 199–207, https://doi.org/10.1016/j.ijmachtools.2005.04.006.
[44] L. Liu, et al., The effect of support on multi-hole drilling for glass fiber-reinforced plastic composite materials, Int. J. Adv. Manuf. Technol. 93 (2017) 953–965, https://doi.org/10.1007/s00170-017-0534-4.
[45] A. Lotfi, H. Li, D.V. Dao, Machinability analysis in drilling flax fiber-reinforced polylactic acid bio-composite laminates, Int. J. Mater. Metall. Eng. 13 (2019) 443–447, https://doi.org/10.5281/zenodo.3455743.
[46] P. Patel, V. Chaudhary, Delamination evaluation in drilling of composite materials–A review, Mater. Today Proc. 56 (2022) 2690–2695, https://doi.org/10.1016/j.matpr.2021.09.267.
[47] A. Faraz, D. Biermann, K. Weinert, Cutting edge rounding: an innovative tool wear criterion in drilling CFRP composite laminates, Int. J. Mach. Tool Manufact. 49 (2009) 1185–1196, https://doi.org/10.1016/j.ijmachtools.2009.08.002.
[48] S. Morkavuk, U. Köklü, K. Aslantaş, An experimental comprehensive analysis of drilling carbon fiber reinforced plastic tubes and comparison with carbon fiber reinforced plastic plate, J. Reinforc. Plast. Compos. 42 (2023) 323–345, https://doi.org/10.1177/07316844221122041.
[49] S. Ahmad Sobri, et al., Augmentation of the delamination factor in drilling of carbon fibre-reinforced polymer composites (CFRP), Polym. (Basel). 12 (2020) 2461, https://doi.org/10.3390/polym12112461.
[50] H. Ho-Cheng, C. Dharan, Delamination during drilling in composite laminates. https://doi.org/10.1115/1.2899580, 1990.
[51] B. Liu, X. Feng, S.-M. Zhang, The effective Young's modulus of composites beyond the Voigt estimation due to the Poisson effect, Compos. Sci. Technol. 69 (2009) 2198–2204, https://doi.org/10.1016/j.compscitech.2009.06.004.
[52] Jr.R.R. Craig, E.M. Taleff, Mechanics of Materials, John Wiley & Sons, 2020.
[53] P. Raval, et al., Energy consumption and economic modelling of performance measures in machining of wire arc additively manufactured Inconel-625, Sustain. Mater. Technol. 32 (2022) e00434, https://doi.org/10.1016/j.susmat.2022.e00434.
[54] C. Kuntz, Perlite: the most sustainable insulation solution for buildings, Perlite Inst (2024). https://www.perlite.org/perlite-the-most-sustainable-insulation-solutionfor-buildings/. (Accessed 18 August 2023).
[55] P.L. Hurtado, et al., A review on the properties of cellulose fibre insulation, Build. Environ. 96 (2016) 170–177, https://doi.org/10.1016/j.buildenv.2015.09.031.
[56] L. Schleisner, Life cycle assessment of a wind farm and related externalities, Renew. Energy 20 (2000) 279–288, https://doi.org/10.1016/S0960-1481(99)00123-8.